Electronic Supplementary Information

Ni Foam Supported NiO nanosheets as High-Performance Free-Standing Electrodes for Hybrid Supercapacitors and Ni-Zn Batteries

Qiang Chen, Jiantao Li, Cong Liao, Guangwu Hu, Yulu Fu, Kwadwo Asare Owusu, Shu Shi, Ziang Liu, Liang Zhou,* and Liqiang Mai*

State Key Laboratory of Advanced Technology for Materials Synthesis and Processing, Wuhan University of Technology, Wuhan 430070, China.

E-mail: mlq518@whut.edu.cn (L. Q. Mai); liangzhou@whut.edu.cn (L. Zhou)

Calculations:

1. NF@NiO Electrode:

The areal capacitances of electrodes were measured by galvanostatic charge/discharge method according to the following equation:

$$C_a = \frac{I \times \Delta t}{\Delta V \cdot S} \qquad (1)$$

where C_a (F cm^{-2}) is the areal capacitance, I (A) is the constant discharging current, Δt is the discharging time, ΔV (V) is the potential window, and S (cm^2) is the surface area.

2. NF@NiO//FeOOH HSCs:

The cell capacitance (C_{cell}) and volumetric capacitance (C_v) of the NF@NiO//FeOOH HSCs were calculated from the slope of the discharge curve using the following equations:

$$C_{cell} = \frac{I \times \Delta t}{\Delta V} \quad (2)$$

$$C_v = \frac{C_{cell}}{V} = \frac{I \times \Delta t}{V \times \Delta V} \quad (3)$$

where I (A) is the applied current, V (cm^3) is the volume of the whole device (The area and thickness of the NF@NiO//FeOOH HSCs device is about 0.5 cm^2 and 0.1 cm. Hence, the whole volume of the NF@NiO//FeOOH HSCs device is ~ 0.05 cm^3), Δt (s) is the discharging time, ΔV (V) is the voltage window. It is worth mentioning that the volumetric capacitances were calculated taking into account the volume of the device stack. This includes the electrode and the separator with electrolyte.

Volumetric energy density, equivalent series resistance and power density of the devices were obtained from the following equations:

$$E = \frac{1}{3600 \times 2} C_v \Delta V^2 \quad (4)$$

$$ESR = \frac{iR_{drop}}{I \times 2} \quad (5)$$

$$P = \frac{\Delta V^2}{4 \times ESR \times V} \quad (6)$$

where E (Wh cm^{-3}) is the energy density, C_V is the volumetric capacitance obtained from Equation (3) and ΔV (V) is the voltage window. ESR (Ω) is the internal resistance of the device. P (W cm^{-3}) is the power density.

3. Balance the charge of electrodes in HSCs device:

As for a SC, the charge balance will follow the relationship $q^+ = q^-$. The charge stored by each electrode depends on the capacitance (C_s), the potential range for the charge/discharge process (ΔE) and the area of the electrode (A) follows the Equation (7):

$$q = C_s \times \Delta E \times m \qquad (7)$$

In order to get $q^+ = q^-$ at 100 mV s^{-1}, the area balancing between NF@NiO and FeOOH electrode will be calculated as follow (8):

$$\frac{A_{NF@NiO}}{A_{FeOOH}} = \frac{C_{A(FeOOH)} \times \Delta E_{(FeOOH)}}{C_{A(NF@NiO)} \times \Delta E_{(NF@NiO)}} \approx \frac{1.03}{1} \qquad (8)$$

The calculated $C_{A(FeOOH)}$ is 0.76 F cm^{-2}, $\Delta E_{(FeOOH)}$ is 1.2 V, $C_{A(NF@NiO)}$ is 1.27 F cm^{-2}, and $\Delta E_{(NF@NiO)}$ is 0.7 V. Therefore, the calculated areal ratio between the NF@NiO electrode and FeOOH electrode is about 1.03 : 1.

4. Ni//Zn battery:

The volumetric capacity C_V (mAh cm^{-2}) was calculated from the discharge curve using the following equations:

$$C_v = \frac{\int_0^{\Delta t} I \times dt}{V} \quad (9)$$

where I (mA) is the applied discharging current, Δt (h) is the discharging time and V (cm^3) is the volume of devices. For the electrodes, the volume is 0.05 cm^3.

Alternatively, the areal capacity of the cell (C_{cell-a})were calculated from the discharge curve using the following equations:

$$C_{cell-a} = \frac{\int_0^{\Delta t} I \times dt}{S} \quad (10)$$

where C_{cell-a} (mAh cm^{-2}) is the specific capacity of the Ni@NiO//Zn battery, I (mA) is the applied discharging current, Δt (h) is the discharging time and S (cm^2) is the total surface area of the Ni@NiO//Zn battery (0.5 cm^2), which is equal to device length (l) by the breadth (b).

Areal energy density E and arealpower density P of the cell were obtained from the following equations:

$$E = C_{cell-a} \times \Delta V \quad (11)$$

$$P = \frac{C_{cell-a} \times \Delta V}{1000 \times \Delta t} \quad (12)$$

where E (mWh/cm^2) is the energy density, C_{cell-a} is the areal capacity obtained from Equation (10) and ΔV (V) is the voltage. P (mW cm^{-2}) is the specific power density and Δt (h) is the discharging time.

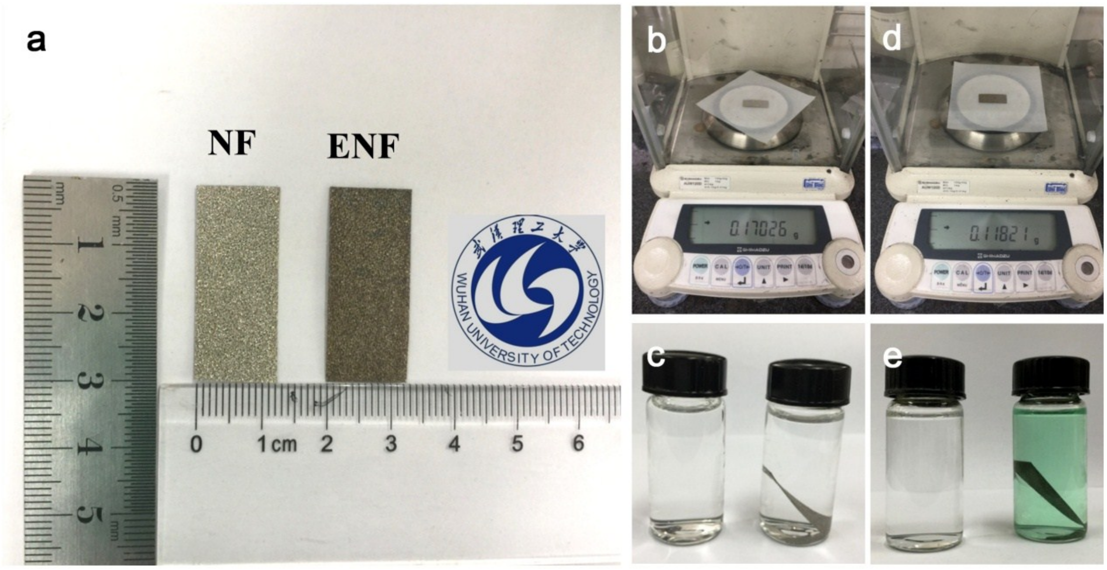

Figure S1. (a) Digital photos of the pristine NF and NF after etching. (b) Weight of the pristine NF. (c) Digital photos of the solutions containing 1.00 M H_3PO_4, 1.00 M $LiCl{\cdot}H_2O$ and 0.05 M KBH_4 without NF (left) and with NF before etching (right). (d) Weight of the NF after etching (NF@NiO). (e) Digital photos of the solutions containing 1.00 M H_3PO_4, 1.00 M $LiCl{\cdot}H_2O$ and 0.05 M KBH_4 without NF (left) and with NF after etching (right).

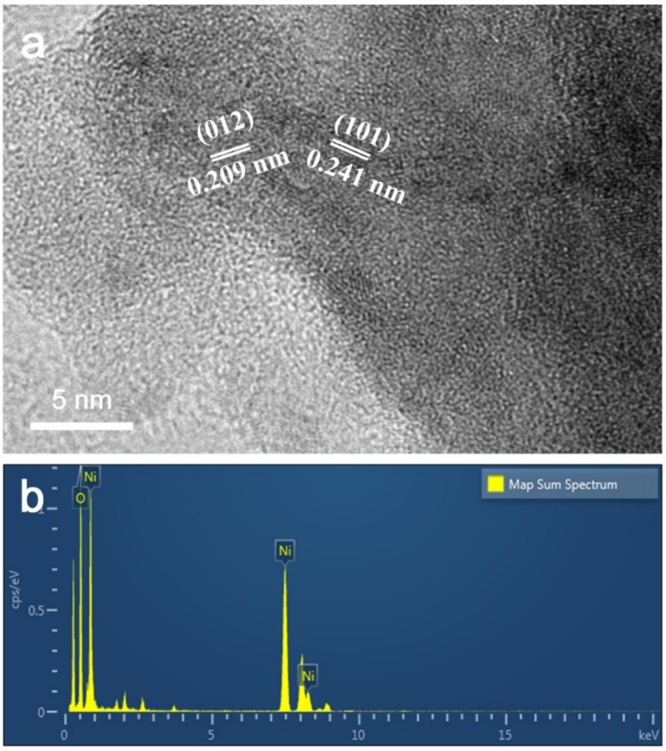

Figure S2. (a) HRTEM image of the NiO nanosheets. (b) EDS spectrum of the NiO nanosheets.

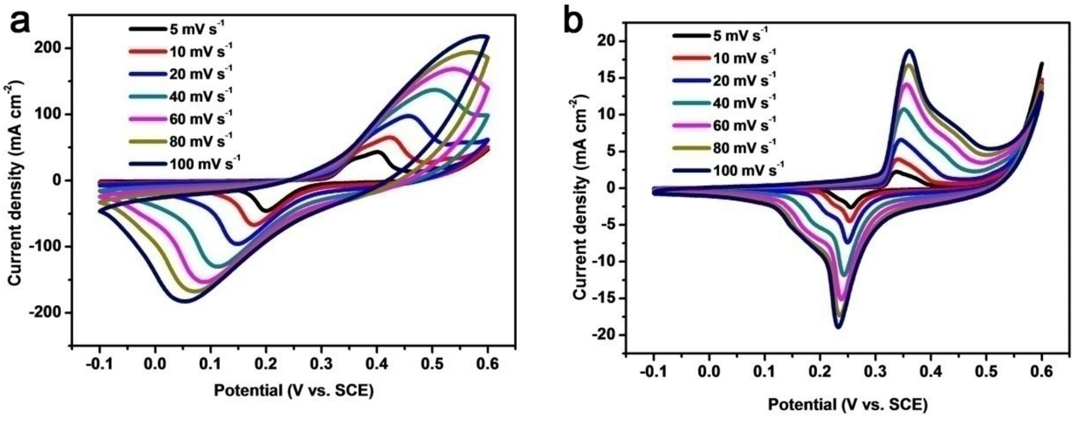

Figure S3. Cycle voltanmmetry curves collected at various scan rates for (a) NF@NiO and (b) NF.

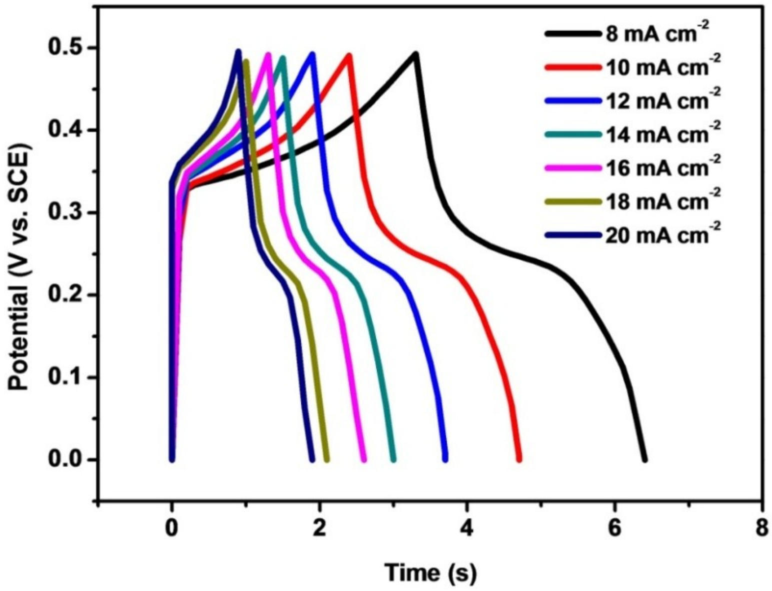

Figure S4. GCD curves of the pristine NF collected at different current densities.

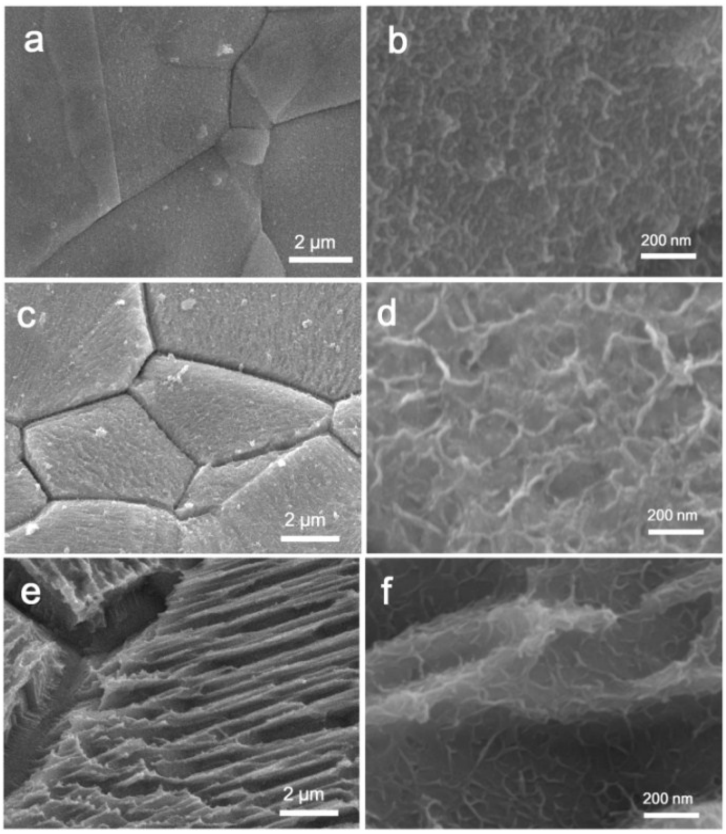

Figure S5. SEM images of NF with different etching time at 120 ^{o}C. (a ,b) 30 min; (c, d) 60 min; (e, f) 180 min.

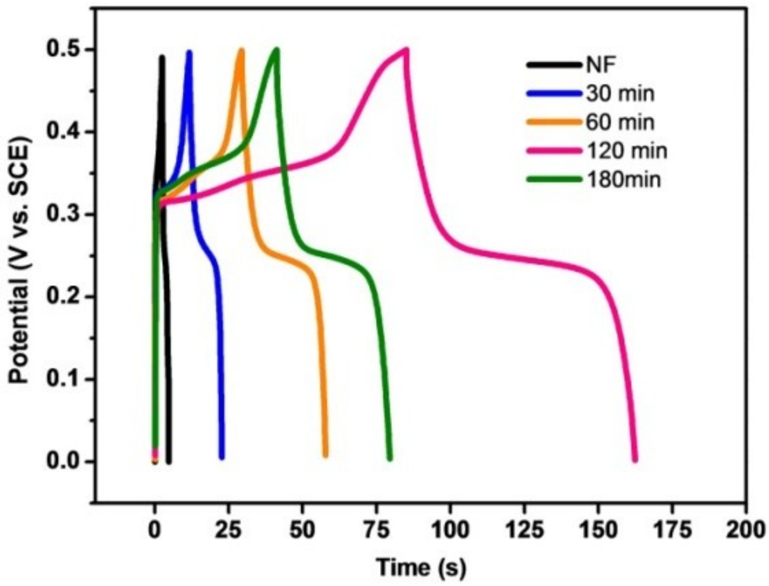

Figure S6. Galvanostatic charge/discharge curves at a current density of 10 $mAcm^{-2}$ for NF with different etching time.

Table S1. Comparison of the capacitance performance of NF@NiO nanosheets to several recently reported state of the art supercapacitors.

Electrode	Morphology	Current density) [mA cm^{-2}]	CP areal capacitance [F cm^{-2}]	Scan rate [mV s^{-1}]	CV areal capacitance [F cm^{-2}]	Substrate	Electrolyte	Reference
NF@NiO [a)]	nanosheets	8	2.01	10	1.30	NF	1.0 M KOH	This work
ANF[a)]	thin film	8	2.04	N.A.	N.A.	NF	6.0 M KOH	S1
$Ni(OH)_2$ [a)]	thin film	2	1.6	N.A.	N.A.	NF	3% KOH	S2
$NiCo_2O_4$@MnO_2 [a)]	nanowires	8	1.91	N.A.	N.A.	NF	1.0 M NaOH	S3
$NiMoO_4$ [a)]	nanoplate	4	1.26	N.A.	N.A.	NF	2.0 M KOH	S4
NiCo-O [a)]	nanowires	5	2.20	N.A.	N.A.	NF	1.0 M KOH	S5
TiN@MnO_2 [a)]	nanowires	2	0.35	10	0.18	CC	5.0 M LiCl	S6
S-V_6O_{13-x} [a)]	nanowires	N.A.	N.A.	10	0.56	CC	5.0 M LiCl	S7
MnO_2@ZnO [b)]	nanorod	N.A.	N.A.	10	0.23	CC	1.0 M	S8
Ti-Fe_2O_3@PEDOT [a)]	nanorod	1	1.15	N.A.	N.A.	CC	5.0 M LiCl	S9

[a)]vs SCE; [b)]vs Ag/AgCl .

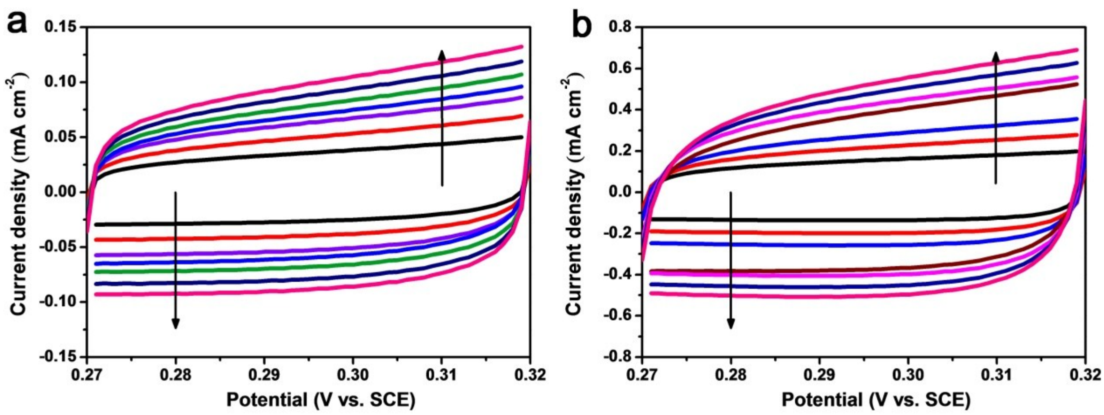

Figure S7. Cyclic voltammograms of (a) NF and (b) NF@NiO in the double layer region at scan rates of 4, 6, 8 10, 12, 14, 16 mV s^{-1} (along the arrow direction).

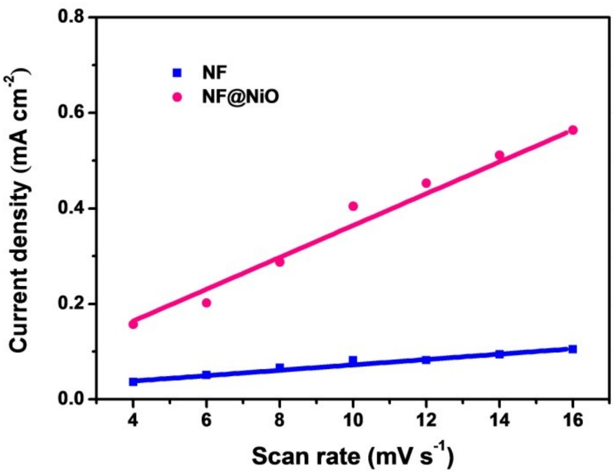

Figure S8. Current density as a function of scan rate for NF and NF@NiO.

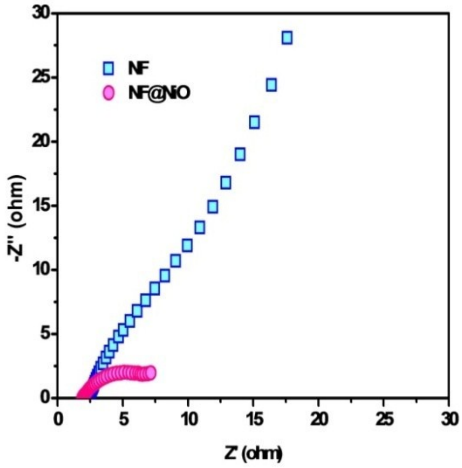

Figure S9. Nyquist plots of NF and NF@NiO collected at 10 mA cm^{-2}.

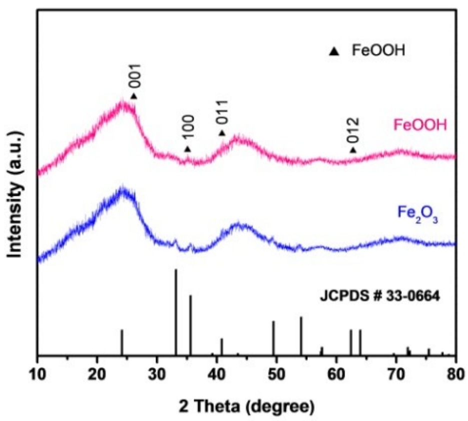

Figure S10. Transformation of α-Fe_2O_3 into FeOOH. XRD patterns of the electrodes before and after electrochemical activation.

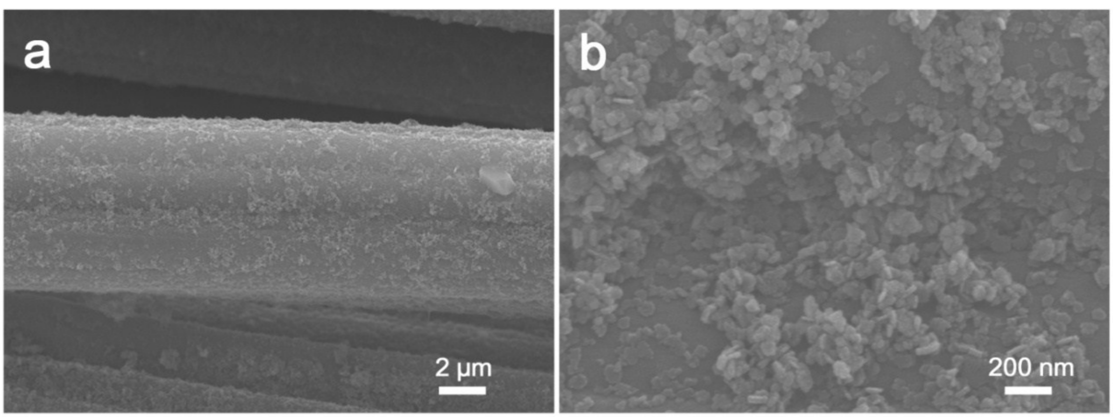

Figure S11. SEM images of FeOOH nanoparticles at different magnification.

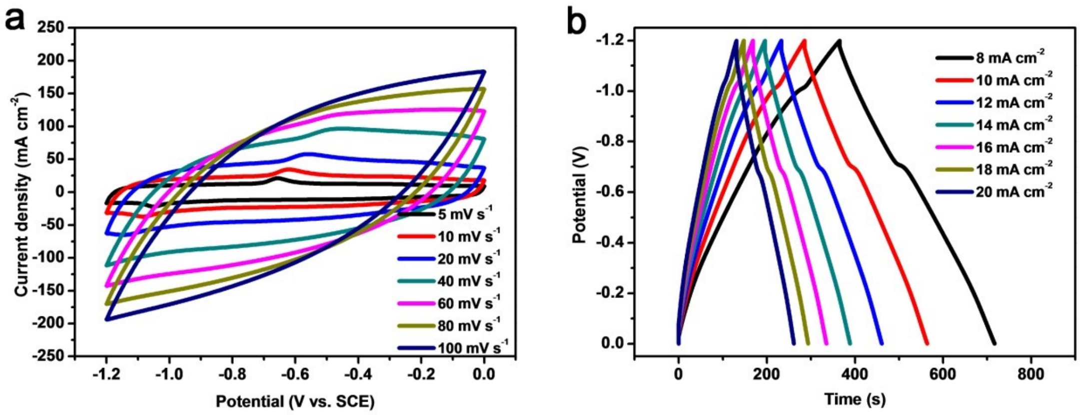

Figure S12. (a) CV curves collected at various scan rates for FeOOH electrode. (b) GCD curves collected at different current for FeOOH electrodes.

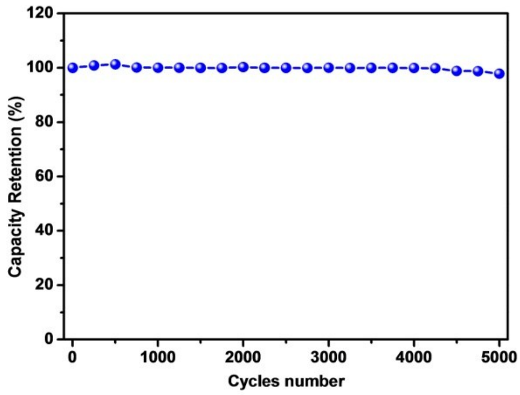

Figure S13. Cycling performance of the FeOOH nanoparticle anode at 10 mA cm^{-2}.

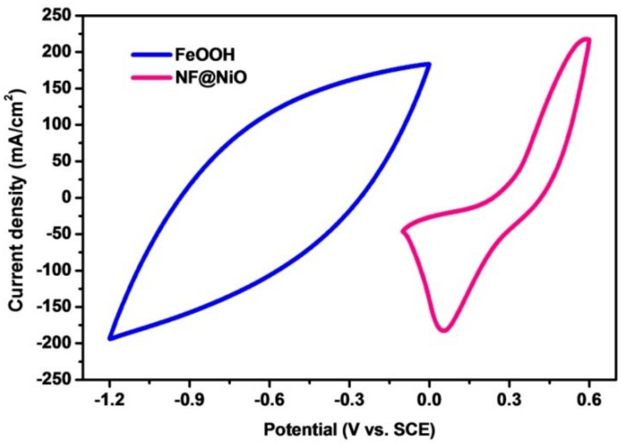

Figure. S14. CV curves collected at 100 mV s^{-1} scan rates for FeOOH and NF@NiO electrode.

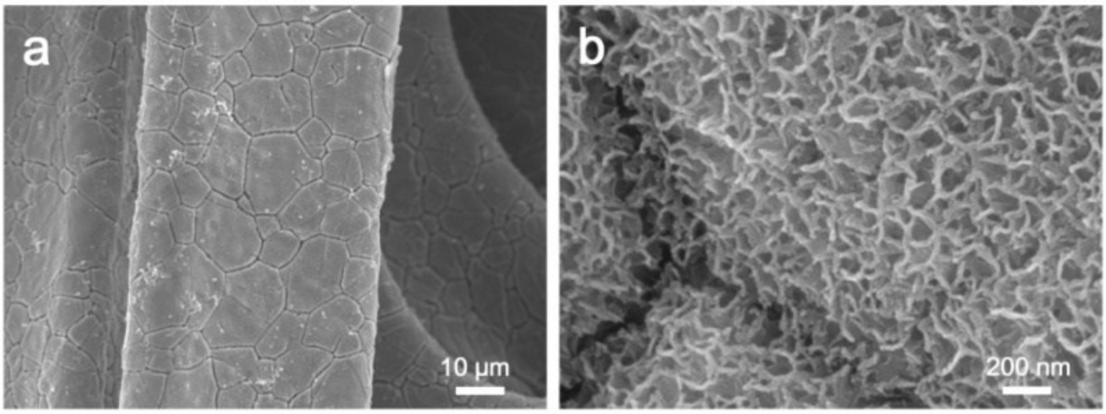

Figure S15. (a) SEM images of NF@NiO after 5000 cycles.

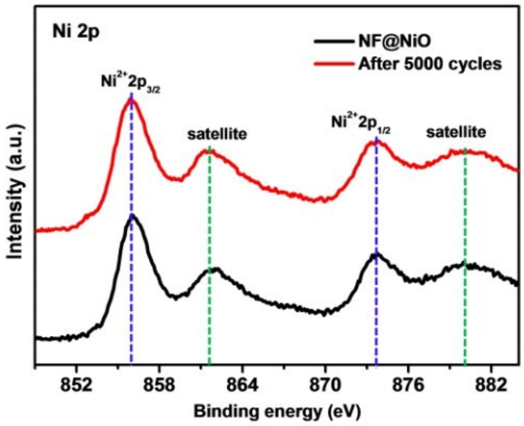

Figure S16. Ni 2p XPS spectra of NF@NiO before and after 5000 cycles.

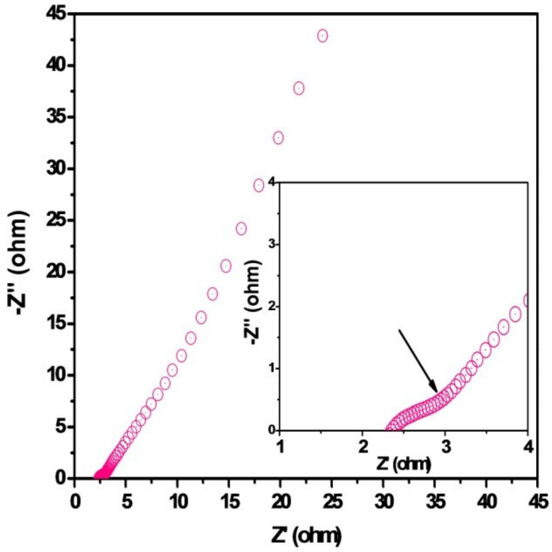

Figure S17. Nyquist plots of the NF@NiO//FeOOH device.

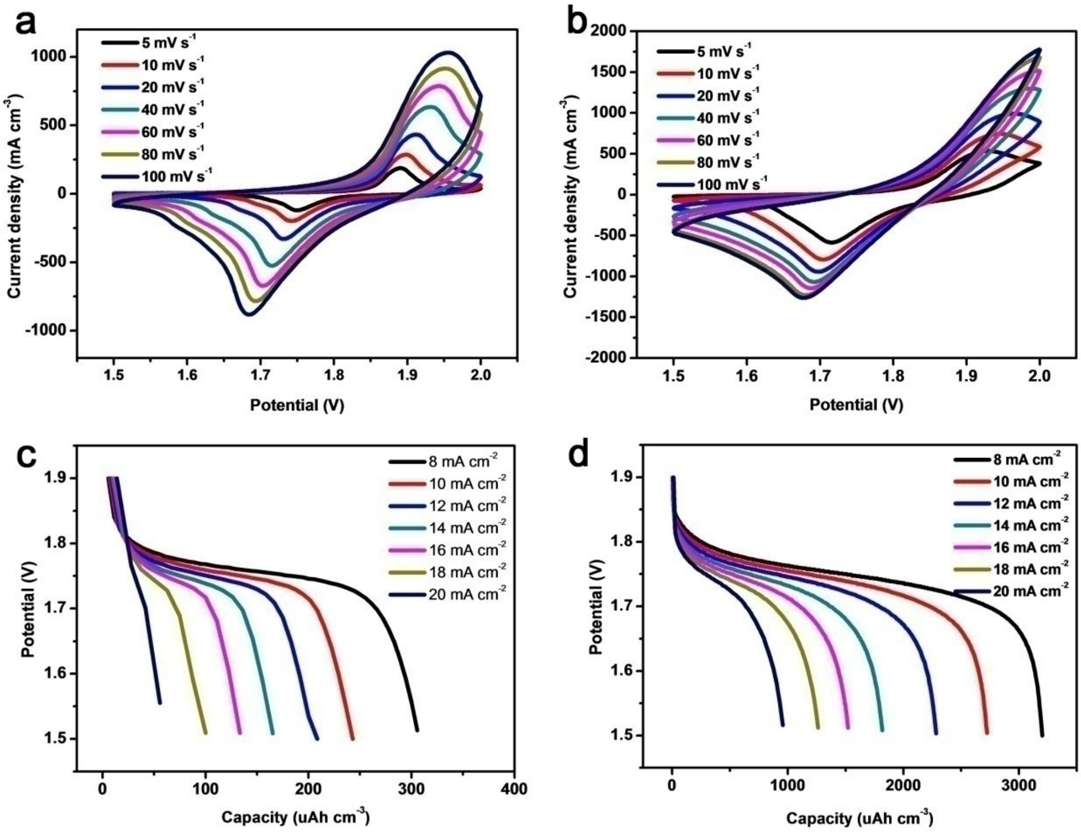

Figure S18. CV curves of the (a) NF//Zn and (b) NF@NiO//Zn batteries at various san rates. Discharge performance of the (c) NF//Zn and (d) NF@NiO//Zn batteries at various current densities.

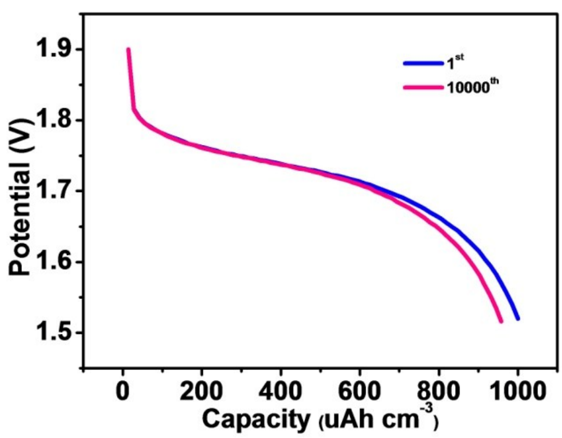

Figure S19. The 1st and 10000th discharge curves collected at 20 mA cm^{-2} for NF@NiO//Zn.

Reference

[S1] M. Yu, W. Wang, C. Li, T. Zhai, X. Lu, Y. Tong, NPG Asia Mater. 6 (2014), e129.

[S2] G. W. Yang, C. L. Xu, H. L. Li, Chem. Commun. 48 (2008), 6537.

[S3] K. B. Xu, W. Y. Li, Q. Liu, B. Li, X. J. Liu, L. An, Z, G. Chen, R. J. Zou, J. Q. Hu, J. Mater. Chem. A 2 (2014), 4795.

[S4] D. Guo, H. M. Zhang, X. Z. Yu, M. Zhang, P. Zhang, Q. H. Li, T. H. Wang, J. Mater. Chem. A 1 (2013), 7247.

[S5] Y. H. Li, L. J. Cao, L. Qiao, M. Zhou, Y. Yang, P. Xiao, Y. H. Zhang, J. Mater. Chem. A 2 (2014) , 6540.

[S6] Y. Liu, R. J. Xiao, Y. F. Qiu, Y. Q. Fang, P. Zhang, Electrochim. Acta 213 (2016) 393.

[S7] T. Zhai , X, H. Lu , Y. C. Ling , M. H. Yu , G. M. Wang , T. Y. Liu , C. L Liang, Y. X. Tong, Y. Li, Adv. Mater. 26, (2014) 5869.

[S8] Z. L. Wang, Z. L. Zhu, J. H. Qiu, S. H. Yang, J. Mater. Chem. C 2, (2014) , 1331.

[S9] Y. X. Zeng , Y. Han , Y. T. Zhao , Y. Zeng , M. H. Yu , Y. J. Liu, H. L. Tang, Y. X. Tong, X. H. Lu, Adv. Energy Mater. 5 (2015) , 1402176.